Block Division for 3D Head Shape Clustering

Jianwei Niu[1], Zhizhong Li[2], and Song Xu[2]

[1] School of Mechanical Engineering, University of Science and Technology Beijing, Beijing, 100083, China
[2] Department of Industrial Engineering, Tsinghua University, Beijing, 100084, China
niujw@me.ustb.edu.cn

Abstract. In our previous Three Dimensional (3D) anthropometric shape clustering study, block-division technique is adopted. The objective of this study was to examine the sensitivity of clustering results on block-division. Such a block-division technique means to divide each 3D surface into a predefined number of blocks. Then by using a block-distance measure, each surface is converted into a block-distance based vector. Finally, k-means clustering is performed on the vectors to segment a population into several groups. Totally 447 3D head samples have been analyzed in the case study. The influence of block division number on clustering was evaluated by using One-way ANOVA. No significant difference was found between the three block division alternatives. This means the adopted method is robust to block division.

Keywords: Three dimensional anthropometry; block-division; clustering; sizing.

1 Introduction

In the past decades, several large scale 3D anthropometric surveys have been conducted, such as Civilian American and European Surface Anthropometry Resource (CAESAR) [1], SizeUK [2], SizeUSA [3], etc. An international collaboration named World Engineering Anthropometry Resource (WEAR) brings together a wealth of different anthropometric data collected across the world [4]. 3D anthropometric shape analysis has found many applications such as in clinical diagnostics, cosmetic surgery, forensics, arts, and entertainment as well as in other fields. How to utilize 3D anthropometric data to improve the fitting level of wearing products has also gained great attention from the ergonomics and human factors [5-14].

An effective way to design fitting products is to analyze the shape of human body forms and classify a specific population into homogeneous groups. Traditionally, some One Dimensional (1D) measurements were usually selected as key dimensions for the analysis of human body variation [15]. Unfortunately, there are some drawbacks in such traditional sizing methods. The most important is that geometric characteristics and internal structure of human surface are not adequately considered, which may lead to design deficiency on fitting comfort [16]. For example, studies have disclosed that foot length and width measures are insufficient for proper fit though most consumers usually select footwear based on the two measurements [17, 18].

V.G. Duffy (Ed.): Digital Human Modeling, HCII 2009, LNCS 5620, pp. 64–71, 2009.

Considering the inherent abundant information contained in 3D anthropometric data, sizing methods based on 3D anthropometric data may be able to overcome the drawbacks of traditional sizing methods. However, this seems not an easy task. In our previous study [19], a block-division method was proposed to convert each 3D surface into a block-distance based vector, which reflects both size and shape difference. Such vectors were then used as the input of k-means clustering algorithm. The influence of the block division number on the 3D shape clustering is further studied in this paper.

The remainder of this paper is organized as follows. Section 2 introduces the proposed method. A case study of 446 3D head samples is then presented in Section 3. Finally, Section 4 concludes this paper.

2 Methods

2.1 Block Division of Head Data

The raw 3D data of 446 head of young male Chinese soldiers (aged from 19 to 23) were collected by a Chinese military institute in 2002 [20]. The data we received are row points of outer surface in each slice. All samples were properly positioned and oriented according to a predefined alignment reference [19].

Once the alignment of a 3D head is done, a 'vector descriptor' is established. A vector descriptor consists of a number of block distances. Here the term of block means a regular patch on the 3D surface. First the inscribed surface of all the samples is calculated. Then the inscribed surface and all sample surfaces can be divided into m blocks. Let P, Q denote the number of the control knots of a surface in u and v directions respectively, and p, q denote the desirable number of the control knots of a block in u and v directions respectively. The control knots of a surface were partitioned into P/p uniform intervals in u direction and Q/q uniform intervals in v direction. Thus the surface was converted into $m = P/p * Q/q$ blocks.

The distance between two corresponding blocks on a sample surface i and the inscribed surface, namely $S(i)$, can then be constructed with two parts, namely $S_1(i)$ and $S_2(i)$, that reflect macro (size) and micro (shape) differences respectively. $S_1(i)$ can be calculated as,

$$S_1(i) = \sum_{j=1}^{n_i} dis(p_{i,j}) \text{ , } i=1, 2, 3,\ldots, m \tag{1}$$

where $p_{i,j}$ is the jth point, and n_i represents the number of points falling into the ith block, and Euclidean distance was used to calculate the distance, dis $(p_{i,j})$, between two corresponding points on the sample and the inscribed surfaces. $S_2(i)$ can be calculated as,

$$S_2(i) = \sum_{j=1}^{n_i} \left| dis(p_{i,j}) - \frac{S_1(i)}{n_i} \right| \text{ , } i=1, 2, 3, \ldots, m \tag{2}$$

S_2 describes the shape variation in the corresponding local areas of two 3D surfaces. Different local areas on a surface can have different shape and geometry characteristics; therefore they contribute differently in the whole shape dissimilarity between a sample surface and the inscribed surface. For example, the geometry of the nose is irregular, so the geometric dissimilarity may play an important role in the total shape dissimilarity between two noses. While the geometry of the upper head is very smooth and quite similar, so the size dissimilarity may play a dominant role in the total shape dissimilarity between two upper heads.

By the above method, the shape of a surface can be characterized by a vector ($S_1(1)$, $S_2(1)$, $S_1(2)$, $S_2(2)$,…, $S_1(m)$, $S_2(m)$). The vectors are the input of the following k-means clustering algorithm.

2.2 Comparison between Different Block Division Numbers

In the case study, each head surface was divided into 20 (5X4), 30 (6X5), and 90 (16X6) blocks, respectively. Then k-means clustering was applied to the block distance-based vectors with different block division number. In this case study, the number of K for the clustering was set as seven.

An evaluation of the influence of the block division number on the clustering results is demonstrated by using One-way ANOVA on the block distance based vectors. The representative head sample of each cluster is obtained first by calculating the average coordinates of the points of the head samples belonging to the cluster. Then the distance between a sample surface and the representative surface can be constructed for $S_1^{'}$ and $S_2^{'}$, respectively. As a prerequisite step of ANOVA, the first examination is whether the $S_1^{'}$ and $S_2^{'}$ display a normal distribution. Tests for normality are conducted on all $S_1^{'}$ and $S_2^{'}$ values using the One-Sample Kolmogorov-Smirnov Test. Another prerequisite step of ANOVA Levene test is to test the homogeneity-of-variance of the variables. Finally, multiple comparisons of means between different block divisions were conducted by using One-way ANOVA.

3 Results and Discussions

3.1 Block Division with Different Block Numbers

The block division results of a head are shown through Fig. 1-3 with block numbers of 20 (5X4), 30 (6X5), and 90 (16X6), respectively. Each block is illustrated with different colors to distinguish from each other. No anatomical correspondence is taken into consideration during the block division. Consequently, as depicted in Fig. 1, it's not surprising that the nose is divided into one block, while both eyes are divided into two different blocks. With the increase of the block division number, the area covered by each block decreases. That's to say, more block division number means fewer points falling into each block.

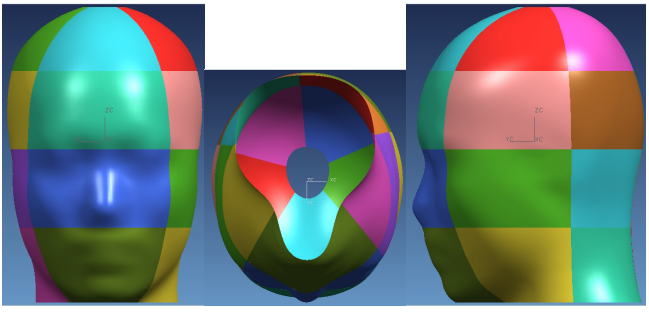

(a) front view (b) bottom view (c) side view

Fig. 1. Block division of a head (20 blocks)

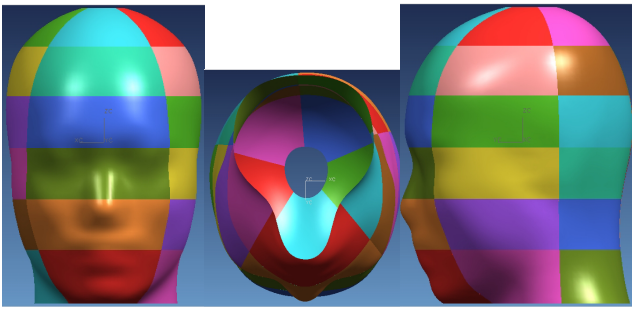

(a) front view (b) bottom view (c) side view

Fig. 2. Block division of a head (30 blocks)

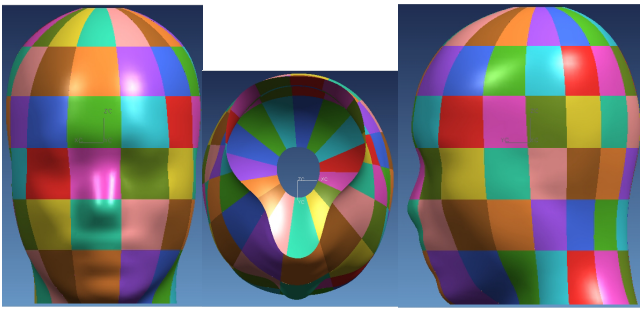

(a) front view (b) bottom view (c) side view

Fig. 3. Block division of a head (90 blocks)

3.2 Clustering Results under Different Block Division Numbers

As shown in Fig. 4, when representative surfaces of clusters are merged together, it is easy to acquire a visual image of the size and shape difference from each other.

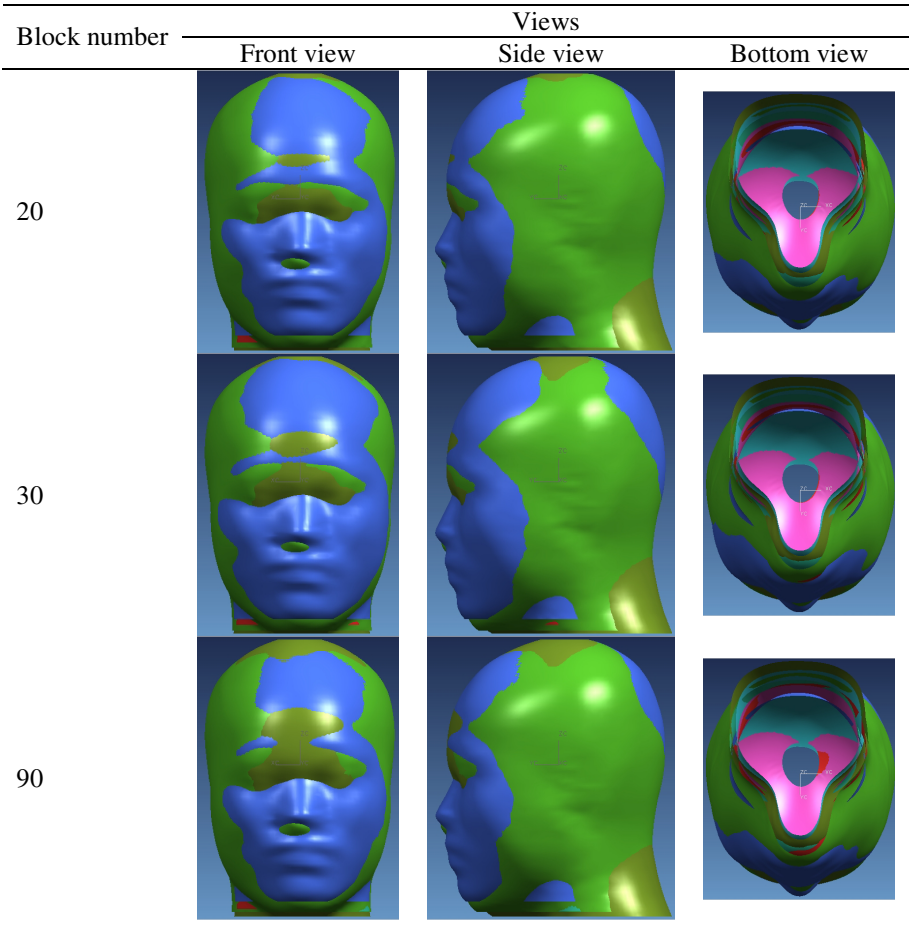

Fig. 4. Different views of the merged average heads of clusters

3.3 Comparison of Results between Different Block Division Numbers

Tests for normality of $S_1^{'}$ and $S_2^{'}$ values showed p values less than 0.05, resulting in rejection of the null hypothesis. Afterwards each $S_1^{'}$ and $S_2^{'}$ values were transformed into their corresponding natural logarithmic values, denoted as $\ln S_1^{'}$ and $\ln S_2^{'}$ respectively. One-Sample Kolmogorov-Smirnov test was conducted on the $\ln S_1^{'}$ and $\ln S_2^{'}$ values, resulting in p values greater than 0.05 (p=0.393 and 0.193 respectively). Levene test on the $\ln S_1^{'}$ and $\ln S_2^{'}$ values showed p values of 0.570 and 0.492, respectively.

As shown in Table 1, One-way ANOVA results demonstrated p values greater than 0.05. Such results lead to no rejection of the null hypothesis. Thus no significant

differences were found between the block division numbers. In other words, this reveals the robustness of the 3D clustering method with block division.

Table 1. Multiple comparisons in One-way ANOVA

Dependent Variable	Group I	Group J	Mean Difference (I-J)	Std. Error	Sig.
$\ln S_1^{'}$	1	2	-.0007	.01967	.971
	1	3	.0156	.01967	.429
	2	3	.0163	.01967	.408
$\ln S_2^{'}$	1	2	.0001	.02102	.997
	1	3	.0004	.02102	.984
	2	3	.0004	.02102	.986

Note: Block division numbers of Group 1, 2, and 3 are 20, 30, and 90, respectively.

Cluster membership variation on different block division number of each sample was investigated and summarized in Table 2. When the block number is changed from 20 to 30 and 90, the numbers of samples whose cluster membership has changed are 10 and 86, respectively (sample size is 446). Whereas, the number of samples with changed membership between 30 and 90 blocks is 88. It can be seen that when the block division number changes within a medium range, the difference of clustering results is almost ignorable. However, when the block division number becomes big, such as 90 in this case study, the membership variation turns to big. This can be explained from the definition of S_1 and S_2 which reflect the local size and shape differences, respectively. When the surface is divided into many blocks, the effect of S_2 is weakened, since for each small block the shape variation is small. Instead, when the block division number is small, the distance of each block is averaged over a big surface, thus the effect of S_1 is weakened; while the shape variation of a big surface is greater, and the effect of S_2 under this situation will be emphasized. Thus too small or great block division number will cause biased consideration of local size and shape.

Table 2. Cluster membership change

Cluster ID	Sample size		
	20 blocks	30 blocks	90 blocks
1	40	39	41
2	71	72	81
3	66	62	76
4	77	78	75
5	63	60	68
6	23	25	27
7	106	110	78
number of change	-	10	86

4 Conclusions

This paper is a further study of our previous 3D shape clustering method based on block division technique [19]. Clustering results of three alternatives of the block division number were compared. One-way ANOVA and cluster membership variation results showed the robustness of the block division method for the k-means 3D shape clustering when the block division number changes within a medium range. However, Extreme block division numbers may lead to greater membership variation.

Acknowledgements

This study is supported by the National Natural Science Foundation of China (No.70571045).

References

1. Robinette, K.M., Blackwell, S., Daanen, H., Fleming, S., Boehmer, M., Brill, T., Hoeferlin, D., Burnsides, D.: CAESAR, Final Report, Volume I: Summary. AFRL-HE-WP-TR-2002-0169. United States Air Force Research Lab., Human Effectiveness Directorate, Crew System Interface Division, Dayton, Ohio (2002)
2. Bougourd, J., Treleaven, P., Allen, R.M.: The UK national sizing survey using 3d body scanning. In: Proceedings of Eurasia-Tex Conference in association with International Culture Festival, Donghua University, Shanghai, China (March 2004)
3. Isaacs, M.: 3D fit for the future. American Association of Textile Chemists and Colorists Review 5(12), 21–24 (2005)
4. WEAR, http://ovrt.nist.gov/projects/wear/
5. Whitestone, J.J., Robinette, K.M.: Fitting to maximize performance of HMD systems. In: Melzer, J.E., Moffitt, K.W. (eds.) Head-Mounted Displays: Designing for the User, pp. 175–206. McGraw-Hill, New York (1997)
6. Elliott, M.G.: Methodology for the sizing and design of protective helmets using three-dimensional anthropometric data. Thesis (PhD). Colorado State University, Fort Collins, Colorado, USA (1998)
7. Meunier, P., Tack, D., Ricci, A., Bossi, L., Angel, H.: Helmet accommodation analysis using 3D laser scanning. Applied Ergonomics 31, 361–369 (2000)
8. Mochimaru, M., Kouchi, M.: Proper sizing of spectacle frames based on 3-D digital faces. In: Proceedings of 15th Triennial Congress of the International Ergonomics Association (CD ROM), Seoul, Korea, August 24-29 (2003)
9. Witana, C.P., Feng, J.J., Goonetilleke, R.S.: Dimensional differences for evaluating the quality of footwear fit. Ergonomics 47(12), 1301–1317 (2004)
10. Zhang, B., Molenbroek, J.F.M.: Representation of a human head with bi-cubic B-splines technique based on the laser scanning technique in 3D surface anthropometry. Applied Ergonomics 35, 459–465 (2004)
11. Witana, C.P., Xiong, S.P., Zhao, J.H., Goonetilleke, R.S.: Foot measurements from three-dimensional scans: A comparison and evaluation of different methods. International Journal of Industrial Ergonomics 36, 789–807 (2006)
12. Hsiao, H.W., Whitestone, J., Kau, T.Y.: Evaluation of Fall Arrest Harness Sizing Schemes. Human Factors 49(3), 447–464 (2007)

13. Lee, H.Y., Hong, K.H.: Optimal brassiere wire based on the 3D anthropometric measurements of under breast curve. Applied Ergonomics 38, 377–384 (2007)
14. Rogers, M.S., Barr, A.B., Kasemsontitum, B., Rempel, D.M.: A three-dimensional anthropometric solid model of the hand based on landmark measurements. Ergonomics 51(4), 511–526 (2008)
15. Gouvali, M.K., Boudolos, K.: Match between school furniture dimensions and children's anthropometry. Applied Ergonomics 37, 765–773 (2006)
16. Li, Z.Z.: Anthropometric Topography. In: Karwowski, W. (ed.) The 2nd edition of the International Encyclopedia of Ergonomics and Human Factors, pp. 265–269. Taylor and Fancis, London (2006)
17. Goonetilleke, R.S., Luximon, A., Tsui, K.L.: The Quality of Footwear Fit: What we know, don't know and should know. In: Proceedings of the Human Factors and Ergonomics Society Conference, San Diego, CA, vol. 2, pp. 515–518 (2000)
18. Goonetilleke, R.S., Luximon, A.: Designing for Comfort: A Footwear Application. In: Das, B., Karwowski, W., Mondelo, P., Mattila, M. (eds.) Proceedings of the Computer-Aided Ergonomics and Safety Conference (Plenary Session, CD-ROM), Maui, Hawaii, July 28-August 2 (2001)
19. Niu, J.W., Li, Z.Z., Salvendy, G.: Multi-resolution shape description and clustering of three-dimensional head data. Ergonomics (in press)
20. Chen, X., Shi, M.W., Zhou, H., Wang, X.T., Zhou, G.T.: The "standard head" for sizing military helmets based on computerized tomography and the headform sizing algorithm (in Chinese). Acta Armamentarii 23(4), 476–480 (2002)